Carbon nanotube reinforced acoustically transparent epoxy nanocomposites for underwater sonar windows

Wei Chen[1,*], Shankar Rajaram[2], Shad Thomas[1], Steven R. Nutt[1]

1. Materials Science and Chemical Engineering, University of Southern CaliforniaVHE406, 3651 Watt Way, Los Angeles, CA, USA, 90089
2. ATS Consulting, 801 South Grand Street, Suite 575, Los Angeles, CA, USA, 90017

Abstract: Oxidized multiwalled carbon nanotubes (o-MWCNTs) were incorporated into filled epoxy blends to develop an acoustically transparent structural nanocomposites for sonar windows. The longitudinal wave speed, density, flexural mechanical properties, loss factor, and insertion loss were characterized for different compositions. The addition of 0.05wt% o-MWCNTs increased the composite flexural modulus and strength by 370% and 90% respectively with no change in the longitudinal acoustic wave speed. Analytical predictions also indicated that higher shear loss factor provided by carbon nanotubes ameliorated shear resonance at oblique insertion angles. Carbon nanotube additions afford the ability to increase mechanical properties and acoustic transparency, both of which are critical for underwater sonar windows.

Key words: Advanced matrix resin development, Nano Materials

*Corresponding author: weichen@usc.edu

1. Introduction

Underwater sonar windows are designed for acoustic transparency and structural integrity, and desirable material characteristics include durability, ease of processing, and consistency. However, the primary design criterion for window materials is sound speed and density that closely match those of seawater [1]. In addition, the material design should minimize dynamic shear modulus,

dilatational loss factor, insertion loss, and maximize the shear loss factor, static shear modulus, tensile modulus, tensile strength, and toughness at the relevant temperature and frequency range (0-50 oC, 1-100KHz).

The available designs of sonar windows have various limitations. For example, sandwich structures are often considered for underwater acoustic applications [2]. However, the acoustic transparency of a sandwich construction can be tuned only to a limited range of frequencies and is accompanied by high insertion loss. This in turn requires a unique design for each application with trade-offs to accommodate the pertinent critical angles of incidence. Consequently, a macroscopic uniform and castable material presents processing and economic advantages over sandwich designs. Thus, non-structural synthetic elastomers, such as polychloroprene rubber, EPDM rubber, and various polyurethanes have been employed in underwater acoustics with sound speed and density that matches water (~1500 m/s, 1000kg/m^3). Such elastomers, however, are compliant and have poor structural rigidity. Alternatively, structural thermosets, such as epoxies, have also been explored as the base material for underwater sonar windows [3-5]. For example, DGEBA epoxies (~2400 m/s) or fluoroepoxies (~1500-2000 m/s) have been compositionally modified with liquid rubber additives, glass microspheres, polymeric micro-balloons, and compliant epoxy pre-polymers to adjust for acoustic and structural properties. These epoxy based composites either suffer from low rigidity and/or high shear resonances, which significantly hamper the direct application for sonar windows. Such limitation highlights the need for an acoustically transparent material or structure that is inclusive of all frequency ranges and insertion angles, while providing structural performance. Recent reports have shown that carbon nanotubes (CNTs) are both efficient reinforcement materials [6-8] and excellent dampers for shear resonance modes in polymer matrices [9, 10], and they may thus offer a means to address both of the issues outlined above. To pursue this possibility, we have

produced thermoplastic toughened epoxy mixtures filled with milled glass fibers, polymeric micro-balloons, and oxidized multiwalled carbon nanotubes (o-MWCNTs) in an attempt to design a castable, macroscopically uniform, inherently damped, and acoustically transparent structural material. The resulting composite exploits the multi-functionality of each ingredient and the flexibility it offers to achieve conflicting design criteria

2. Theory

In acoustically transparent materials, or structures, acoustic energy can enter and pass through the materials, or structures, without significant losses due to reflection and attenuation. For underwater applications in which incident sound waves impinge perpendicular to the surface, formulations for acoustic transparency in water require that the product of the density and longitudinal wave speed, or acoustic impedance Z_0 (Eqn. 1), matches that of water**.** However, for applications that require an insertion angle other than 0^o, density and sound speed should be matched with water individually, a requirement that is expressed as

$$\boldsymbol{Z_0 = \rho \times c} \qquad (1)$$

Z_0 : acoustic impedance

ρ: density

c: wave speed

For acoustically transparent structures, inherent damping that minimizes radiated energy without affecting sound transmission is also essential. A high dilatational loss factor, increases transmission loss (TL) and thus must be minimized. However, increasing the shear modulus loss factor dramatically reduces the amplitude of the TL peaks. Hence, the real challenge in the design

of sonar windows is to maximize the shear modulus loss factor while maintaining a low dilatational loss factor. This allows the material to damp out the shear waves generated and also minimize destructive interference between shear waves and longitudinal waves.

CNTs exhibit high aspect ratios and superb mechanical properties [11], and are thus considered as ideal reinforcement materials [12, 13]. On the other hand, for acoustic considerations, conventional fillers such as glass fibers and phenolic micro-balloons can either increase modulus at the cost of increasing wave speed or decrease the modulus while also reducing the wave speed. Because of their small size, CNTs can exert relatively small effects on acoustic waves at the frequency ranges of interest. Furthermore, carbon nanotubes additions inherently dampen the shear modes of the material by improving the shear loss factor without altering the dilatational loss factor through a stick-slip mechanism at carbon nanotube-polymer interface [9, 10]. Suhr and coworkers [9] pointed out that multi-walled carbon nanotubes (MWCNTs) increase the shear modulus loss factor up to 1400% at low frequencies without sacrificing the storage modulus. Carbon nanotubes and carbon nanofibers were also reported to enhance damping effectively at higher frequencies and in stiffer matrices [14, 15].

3. Formulation

Acoustic transparency can be engineered by inclusion of CTBN [3], aliphatic epoxy pre-polymer [4], and phenolic micro-balloons [1, 4] to reduce wave speed and density, and subsequently adjusting the structural properties by the addition of reinforcing fillers such as glass fibers and o-MWCNTs. While the addition of milled glass fibers will increase the sound speed, density, and modulus of the composites, the addition of compliant components, specifically, rubber based

additives (CTBN), and the phenolic micro-balloons, will have a compensating effect. In the present work, formulations were based on the above principles and the key samples are listed in Table 1 as A through H, with control sample N_0.

Table 1. *Formulation of Test Samples*

	EPON828 (phr)	DER732 (phr)	2,4 - EMI[1] (phr)	CTBN (phr)	MWCNT[2] (wt%)	Phenoset (wt%)	Glass Fiber (wt%)	Nano-clay (wt%)
N_0	100	0	3	--	--	--	--	--
A	100	0	3	20	--	--	--	--
B	100	0	3	20	0.05	--	--	--
C	75	25	3	20	--	--	--	--
D	75	25	3	20	0.05	--	--	--
E	75	25	3	20	0.50	--	--	--
F	60	40	3	20	--	--	--	--
G	60	40	3	20	0.05		--	--
H	60	40	3	20	0.05	2	--	--
I	60	40	3	20	0.05	2	--	2.5
J	60	40	3	20	0.05	2	2	2.5

Note:
[1] 2, 4 -EMI was used as curing agent for all system listed.
[2] MWCNTs were oxidized before use.

Three approaches were employed to control the wave speed of the DGEBA epoxy system. First, the base epoxy backbone was varied from rigid to compliant by varying the proportions of the aromatic diglycidyl ether of bisphenol-A (DGEBA) epoxy monomer, EPON828, and the aliphatic monomer, DER 732. The rigidity of the epoxy sample was varied by blending the compliant DER732 aliphatic epoxy at 0, 25, and 40 parts per hundred resin (phr) to DGEBA. The rigid systems used 100 phr EPON828, while semi-rigid systems used 75 phr EPON828 and 25 phr DER 732. The compliant systems used 60 phr EPON828 and 40 phr DER 732. Each of the formulations also

included an elastomeric modifier (carboxyl terminated butadiene acrylonitrile, CTBN) to reduce the wave speed and increase toughness of the epoxy systems [3]. CTBN dissolved in the epoxy resin when mixed at elevated temperature, although during subsequent curing, it phase-segregated into micron-sized spherical rubbery domains, which enhanced the toughness and elongation of the resulting material. Finally, phenolic micron-balloons with an average density of 314 kg/m^3 (Phenoset, supplier), were added to adjust the density and meet the design criteria. According to Thompson [1], the addition of polymeric micro-balloons will decrease composite density substantially and decrease wave speed moderately.

Milled glass fibers (1/16") and o-MWCNTs were added to increase the strength and modulus of the polymer composites. The reinforcing behavior of short-fiber-reinforced polymer composites can be estimated by the Halpin-Tsai or Mori-Tanaka model [16, 17]. Glass fibers increase the modulus of the composites at the cost of higher acoustic wave speed, similar to that observed for glass micro-spheres [1]. Oxidized MWCNTs were added in samples B, D, E, G, H, I, and J. The oxidization process introduced carboxylic, carbonyl, and hydroxyl groups on to MWCNT surface. These surface functionalities provided cross-linking sites that enhanced the interfacial stress transfer properties at the MWCNT/matrix interface, while simultansiouly enhancing the dispersion of the nano-fibrils. In a parallel study conducted in this work, the role of o-MWCNTs as a non-intrusive reinforcement for underwater acoustics was investigated utilizing the base epoxy formulation (N_0) filled with o-MWCNT of 0.01, 0.025, 0.05, 0.075, 0.1, 0.5, 1, and 2 wt% respectively.

The surface-modified nano-clay garamite was used as an anti-settling agent (ASA) to prevent phase separation and microsphere flotation or migration by increasing the viscosity or

enhancing shear-hardening properties of the mixture. The nano-clay also served as a reinforcement component in the formulation.

All samples were prepared in a dual-axis, high-speed mixer (Keyence, HM501) to provide high shear force and attain uniform materials dispersion. Three-minute degassing was performed in the same mixer after each mixing step to remove air bubbles generated during mixing. The following general sample preparation procedures were employed: First, DER732 was mixed with EPON828 for 5 min, and then CTBN was introduced at 150 ^{o}C and mixed for minimum 1 hr to attain a uniform mixture.The mixture was then cooled to room temperature. Afterwards, milled oxidized MWCNTs were added and the resultant mixture was sonicated for 30 minutes (Aquasonic, 150D, VWR Scientific) and mixed for 5 min. Subsequently, nano-clay, phenolic micro-balloons, glass fibers, and the curative were mixed (5 min) and degassed (3 min) separately in that order. Finally the mixture was cast into an aluminum mold pretreated with releasing agent and cured. All samples were cured at 65 ^{o}C for 24 hours and post-cured at 120 ^{o}C for 3 hours. Small specimens were cut for subsequent measurements. The final scaled-up sample (45.72cm x 45.72 cm x 1.27 cm) was made in sub-batches, and each batch weighed approximately 170g due to the sample size limitation of the hybrid mixer.

4. Experiments & Model

Pulse-echo measurements (Figure1a) were performed in a standard NDT ultrasonic immersion tank at 5 MHz to estimate the longitudinal wave speed of the material at 25 ^{o} C in fresh water. For samples with phenolic microspheres, pulse-echo tests were not viable due to the absorption of frequencies ~5 MHz associated with the microspheres. Therefore, a free-free

excitation set-up was also used for longitudinal wave speed measurement, as shown in Figure 1b. The free-free beam measurements were used to excite column resonances for determination of the compressional wave speed and agreement between these two methods were established for samples tested with both approaches.

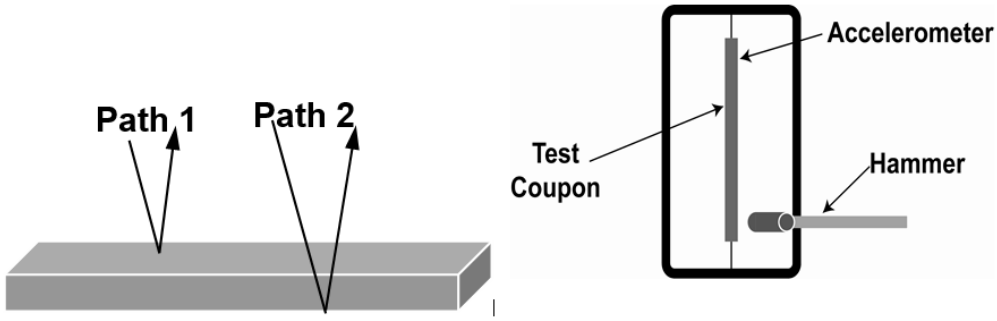

Figure 1. *Pulse-echo method (a) and free-free beam measurement (b) for longitudinal wave speed test*

Clamped-free slender beam excitation was used to determine values of elastic and shear modulus. The complex moduli were based on the relations:

$$E' = E\left(1 + i\eta_E\right) \tag{2}$$

$$G' = G\left(1 + i\eta_G\right) \tag{3}$$

$\eta_E - elastic loss\ factor$

$\eta_G - shear loss\ factor$

The average for the lowest 4 to 5 modes was used to determine the loss factors. The elastic and shear loss factors were determined by measuring the bandwidths of the individual bending and torsional beam resonances respectively. The Young's modulus and shear modulus used in Eqn. 2, 3 were estimated using the following relationships:

Young's modulus:

$$E = 12\rho\left(\frac{l^4}{a^2}\right)\left[\frac{\omega_n}{(\beta l)_n^2}\right]^2 \tag{4}$$

Shear modulus:

$$G = \frac{\rho l^2 (a^2 + b^2) \omega_n^2}{3\pi^2 (2n-1)^2 b^2 k_1} \quad (5)$$

$l = Length$

$a = Thickness$

$b = Width$

$\rho = Density$

$(\beta l)_n = \left(\frac{2n-1}{2}\right)\pi$

$k = Shape\ Factor\ (0.281)$

The ω_n values used in Eqn. 4, 5 were typically for the first mode. The expressions shown for *E* and *G* do not account for rotary inertia and shear-deformation effects. These effects become increasingly noticeable as the mode number increases.

The flexural tests were performed on a universal testing machine using a three-point bending fixture to obtain the flexural modulus and flexural strength values according to the ASTM D790M at a strain rate of 1 s^{-1}. Five beam-shaped specimens were cut and polished for each test. Densities of the samples were measured with a pyconometer.

Dynamic mechanical analyses (DMA, TA Instruments) were performed to monitor the changes of the glass transition temperature (T_g), storage moduli (E'), and loss modulus (E") in the composites from 25°C to 150°C at a heating rate of 5°C per minute and load frequency of 1 Hz.

The acoustic performance of the scaled-up panel was tested at the underwater insertion loss facility of the US Navy's NUWC Division at Newport, RI (APTF). The insertion loss of the panel was measured at a distance of 2 meters at the centerline of the test tank in 20 ^{o}C fresh water. Insertion loss was scanned between 10 and 100 KHz at normal incidence (0^o) and at both, 15^o, and 30^o off normal incidence.

The acoustic performance for sonar windows was defined in terms of a plane wave Transmission Loss (TL) and was predicted using a finite element model of a submerged, planar, isotropic, viscoelastic layer of infinite extent. The following input parameters were used for the window material based on measurements of the final sample (J). The window thickness was taken as 1.27 cm, the same as the final scaled-up panel. The nominal density and sound speed of water was taken to be 1000 kg/m^3 and 1500 m/s respectively.

5. Results & discussion

5.1 Wave speed reduction and density adjustment

The measured wave speed, density, and flexural properties are shown in Table 2. Because of the buoyant migration of phenolic micro-spheres, test results for sample H were not recorded. The incorporation of liquid rubber additive (CTBN), compliant aliphatic epoxy pre-polymer, and phenolic micro-spheres reduced the wave speed (and density) to values comparable to fresh water (~1500m/s).

Table 2. *Wave speed and Static Mechanical Properties of the Samples*

Sample	Wave Speed (m/s)	Flexural Properties (MPa)		Density (kg/m^3)
		Modulus	Strength	
N_0	2480	2800	78	1158
A	2200	734	56	1112
B	2130	1126	45	1109
C	1910	92	8	1099
D	1935	430	15	1101
E	1922	97	12.5	1117
F	1799	34	2	1093
G	1783	325	6	1095
H	--	--	--	--
I	1702	462	9.5	920
J	1750	600	14	980

The CTBN-toughened specimen B (20 phr) exhibited a 4% decrease in density and an 11.3% decrease in wave speed compared with the control specimen N_0. Ramotowski [3] reported that CTBN additions also increase both toughness and elongation of the composite. Although flexural properties decreased, the resulting sample exhibited acoustic properties superior to other castable polymers of similar modulus at room temperature, a factor attributed to the acoustic impedance matching with water.

Blends containing higher concentrations of DER732 were more flexible. A reduction in wave speed of 100-120 m/s for every 10 phr of flexible epoxy inclusions was observed for all samples affected. Sample density reduction was also negligible. Blends rich in DER732 may be suitable as potting materials but lack the mechanical strength and rigidity required for sonar window

applications. However, an efficient non-intrusive reinforcing material would make these formulations suitable for acoustic window applications.

The acoustic impedance can be more closely matched by reducing density through the addition of phenolic micro-balloons. While the addition of micro-balloons altered the density match with water and slightly decreased the wave speed and mechanical properties [1, 4], the combined effect of phenolic micro-balloon and nano-clay effectively reduced composite density while enhancing the mechanical properties by 30-50%.

5.2 Reinforcement effect of fillers

Although the composite wave speed and density were effectively reduced by the additions of CTBN, aliphatic epoxy, and phenolic microspheres, the mechanical properties were degraded. Thus, milled glass fiber, nano-clay, and o-MWCNTs were employed to enhance the mechanical properties, resulting in different reinforcing efficiencies. Interactions between fillers were assumed to be negligible in terms of the reinforcing effects.

Garamite nano-clay was included in formulations I and J as an anti-settling agent, and caused an increase strength and stiffness, an effect opposite to the effect of adding phenolic micro-balloons. Both the flexural modulus and strength increased 30-50% for specimen I (compared with sample G), a phenomenon attributed to the inclusion of 2wt% of surface modified nano-clays. However, the longitudinal wave speed does not conform to the square root rule of the wave speed – modulus correlation (Eqn. 6) based on specimens G and I, and this effect was attributed to the nano-scopic clay reinforcement used. The classical relationship described in Eqn. 6 is not suitable for heterogeneous materials with nano-scale reinforcements.

$c = (E/\rho)^{1/2}$ (6)

E: modulus

ρ: density

Milled glass fibers (1/16") were also used to increase the mechanical properties in sample J. The increase in stiffness observed for J compared to I is attributed to the addition of 2% glass fibers. The wave speed of the composite also increased by 20-25 m/s per wt%, an effect similar to that observed for glass micro-spheres[1, 18]. In addition, the density of sample I was also increased slightly to provide a closer match to fresh water.

The longitudinal wave speed, density, glass transition temperature (T_g), and storage modulus were measured and compared for each sample to determine the role of o-MWCNTs. As shown in Figure 2, o-MWCNT additions provided additional reinforcement without affecting the longitudinal wave speed. The storage modulus increased ~20%, while the longitudinal wave speed was largely unaffected. The behavior of composites with o-MWCNTs deviated from Eqn. 6 (just as with nano-clay systems), and the deviation was attributed to vast difference in length scales for MWCNTs compared with the acoustic wavelengths. Both the storage modulus and the glass transition temperature peaked at 0.05wt% for oxidized MWCNT (Figure 2a). At higher nanotube loadings, the decrease in both storage modulus and glass transition temperature resulted from o-MWCNT agglomeration and the exponential increase in viscosity during processing [6, 7]. The dispersion of o-MWCNTs, and thus the reinforcement efficiency, was partly limited by the processing methods. With optimized dispersion techniques, carbon nanotube additions are expected to cause the modulus and strength of the composites to increase by orders of magnitude[8] without affecting the longitudinal wave speed.

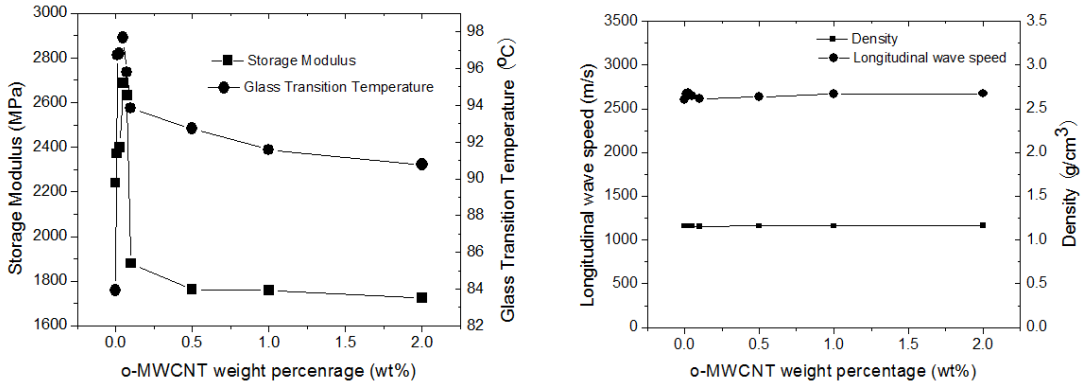

Figure 2. *Test results of neat MWCNT reinforced epoxy composites with Various CNT Filler Concentration*

The results of samples A through J showed that o-MWCNTs imparted greater reinforcement efficiency for matrices with lower modulus. For example, in the stiff epoxy systems (sample A, B), addition of 0.05wt% o-MWCNT increased the flexural modulus and strength by 53% and 19%. On the other hand, in the semi-rigid systems (C, D, and E), the addition of 0.05 wt% o-MWCNT caused the modulus to increase by 370% and the strength to increase by 90% (Figure 3). However, composites with higher CNT content (0.5wt% o-MWCNT, sample E) exhibited a reduction in flexural strength and modulus relative to specimens with lower nanotube loadings. Finally, the greatest reinforcement efficiency was observed for the most compliant matrices (G, I, J) where both strength and modulus values increased several-fold after additions of 0.05wt% o-MWCNT.

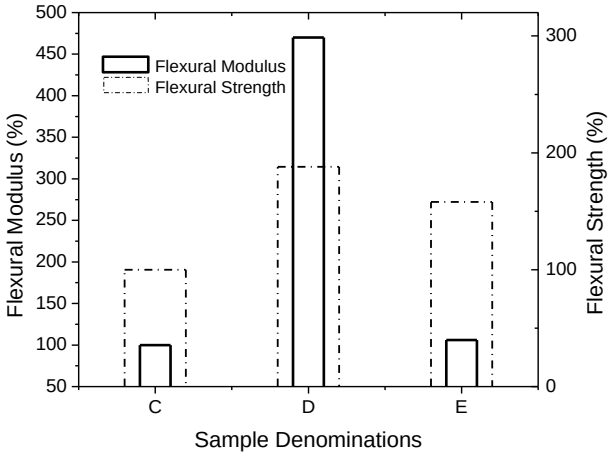

Figure 3. *Flexural Modulus & Flexural Strength of epoxy elastomer blends*

The properties of the scaled-up sample are listed in Table 3. The wave speed of the final composite was reduced by 30% from the original DGEBA epoxy composition, while the density was 980 kg/m^3, nearly matching that of fresh water. The mechanical properties of the final sample increased significantly compared with sample F. Further improvements in dispersion, alignment, and interface control of CNT-reinforced composites will be key elements in future research in order to realize the full reinforcing effects of CNTs.

Table 3 *Final Sample Properties*

Wave Speed	1750 m/s (estimate from free-free beam excitation))
Density	980 kg/m3
Tg	Below room temperature (25 ^{o}C)
Static Modulus	600 MPa (3-point bending)
Strength	14 MPa (3-point bending)
Failure Strain	11% (3-point bending)
Elastic Modulus	1290 MPa (Clamp-free slender beam excitation)
Shear Modulus	440 MPa (Clamp-free slender beam excitation)
Dilational Loss Factor	0.048 (Clamp-free slender beam excitation)
Shear Loss Factor	0.049 (Clamp-free slender beam excitation)
Poisson's Ratio	0.45 (Clamp-free slender beam excitation)

5.3 Transmission Loss

The measured insertion loss data on the final scaled-up panel at 0, 15, and 30 degrees of incidence are illustrated in Figure 4.

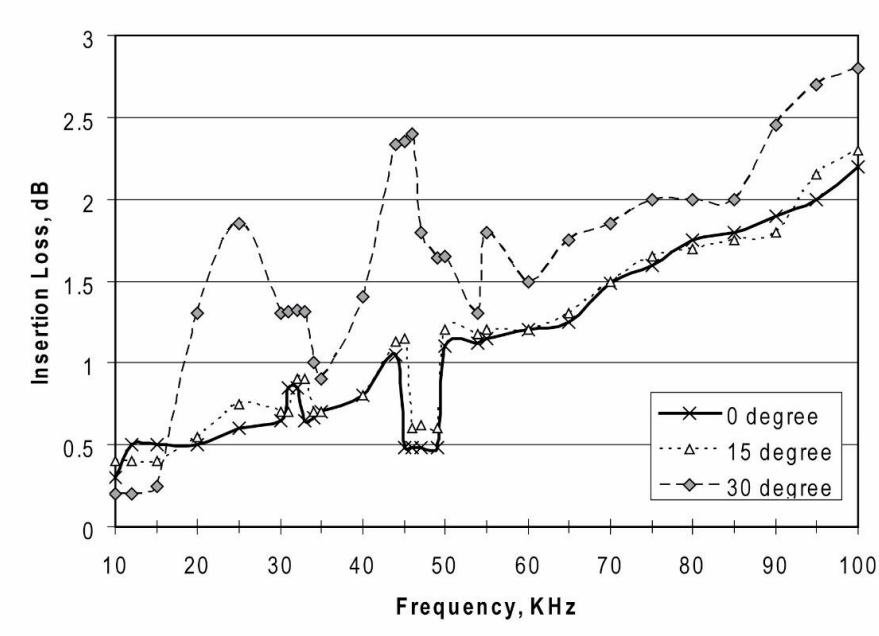

Figure 4. *Measured Insertion Loss at Various Angles of Incidence.*

Insertion loss at 0^o and 15^o incidence increased linearly with frequency and was less than 3 dB over the frequency range 10-100 KHz for 0 (normal), 15, and 30 degree incidence. The drop in insertion loss between 45-50 KHz is a testing artifact. The results show an insertion loss peak at 25 KHz that increases as the angle of incidence deviated from the normal incidence. At 30 degree incidence, the peak occurs at 25 KHz, which is the frequency at which the panel thickness measures one-half the shear wavelength. The frequency of the insertion loss peaks is dependent on the panel thickness, the density match to the water medium, the boundary conditions of the panel and the lateral dimensions of the panel. The magnitude of this shear resonance peak is controlled by the shear modulus of the composite, the panel thickness and the angle of incidence. The increase in peak magnitude with angle of incidence is expected, because for any given panel, the effective thickness of the panel increases with incidence angle. Consequently, more incident energy is converted into shear modes when the effective thickness of the panel is higher. This results in more prominent insertion loss peaks at higher angles of incidence.

The insertion loss (IL) of the panel was simulated as a function of frequency at different angles of incidence. Because the trends indicated by IL were qualitatively equivalent to the TL trends and TL analytical tools were readily available, TL predictions were used to study the role of CNT damping in enhancing acoustic transparency. The analytical model for predicting the Transmission Loss (TL) of the panel was two-dimensional and planar. The window material was embedded in an infinite acoustic medium and represented as a homogeneous and isotropic viscoelastic layer of given thickness and infinite extent. It was thus defined by its thickness, its mass density and two elastic (Lame's) constants, taken to be complex to model dissipation in the material. A plane, harmonic, acoustic wave, pi(q;w), was assumed to be incident on the panel at an arbitrary angle (q) to the panel normal, and the portion of the wave transmitted across the panel, pt(q;w), was computed. In turn, TL values were defined as:

$$TL=-20\log| pt(q;w)/pi(q;w)| \quad (7)$$

Results of TL predictions from the analytical model are plotted in Figure 5 from 1-40 kHz, from normal incidence ($\theta = 0^{o}$) to near grazing ($\theta \to 90^{o}$).The TL values are less than 1 dB for frequencies less than 10 KHz for all incidence angles below 60^{o}. The TL also peaked at 25 KHz, which coincides with the measured IL data. Thus, the predicted TL qualitatively agrees with the insertion loss measurements of the fabricated panel. The qualitative similarity serves as partial validation of the model and establishes the utility for predicting the TL trends of newer/hypothetical formulations.

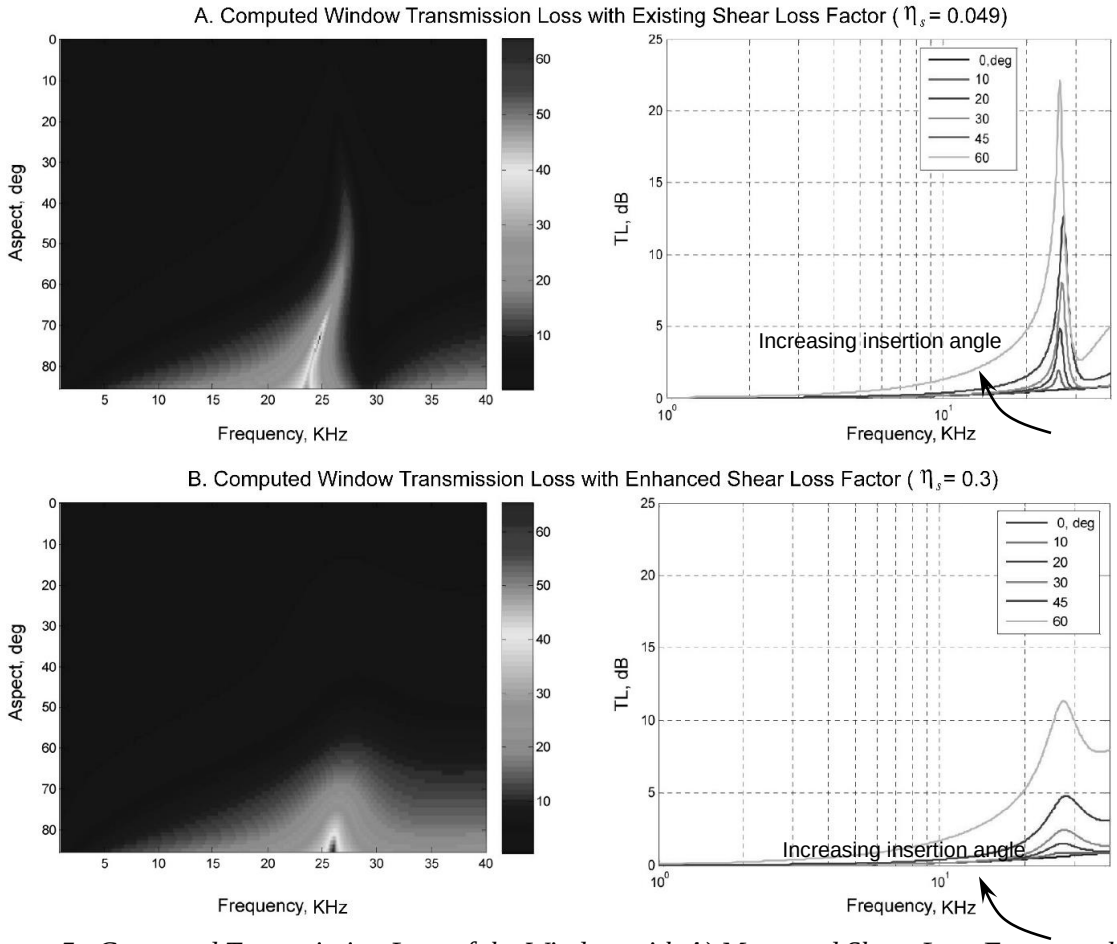

Figure 5. *Computed Transmission Loss of the Window with A) Measured Shear Loss Factor and B) Assumed Shear Loss Factor due to Carbon Nanotube Damping.*

The shear resonance associated with the panel thickness can be ameliorated by increasing the shear loss factor of the material. (For materials with Poisson's ratio one, this increase in damping will somewhat degrade performance at other frequencies that are influenced by shape factors other than panel thickness.) The introduction of carbon nanotubes can directly affect the shear loss factor, thus offering a possible solution to this design dilemma. Current measurements of the shear loss factor of the final sample are close to the dilatational loss factor, ~ 0.048, and this effect is attributed to the additions of CTBN and phenolic micro-balloons, not CNTs. The reason is two-fold: First, shear damping occurs only selectively under a stick-slip mechanism, and the energy dissipated is dependant on the surface area of the nano-filler involved. Thus, the selective damping at shear modes

may be realized only at higher CNT concentrations. Second, the functionalization of CNT surfaces promotes cross-linking at CNT surfaces and enhances uniform CNT dispersion in the epoxy. Furthermore, it increases the interface shear modulus, and thus suppresses the stick-slip mechanism necessary for shear mode damping. With improved dispersion methods and controlled CNT surface condition, CNT additions could reduce shear resonance effectively even at higher CNT loadings. To illustrate this hypothesis, the shear loss factor was increased from $\eta_s = \eta_d = 0.049$ to $\eta_s = 0.3$ (500% increase as a conservative estimate) and the TL was predicted (see Figure 5b). The predicted TL trends show a significant suppression of the TL peaks even at higher angles of incidence for the shear loss factor of 0.3. This demonstrates that selective CNT damping can improve the acoustic transparency of monolithic panels for a wide range of incident angles.

6. Conclusions

Epoxy pre-polymers were copolymerized to synthesize matrices for acoustically transparent composite materials for underwater sonar windows. CTBN, phenolic micro-balloons, glass fibers, nano-clay, and o-MWCNTs were incorporated into the epoxy system, and the acoustic behavior and mechanical properties of each composition was measured and analyzed.

The addition of o-MWCNT significantly increased the strength and modulus of the composite without affecting the longitudinal wave speed. Thus, carbon nanotubes show promise as an efficient non-intruding reinforcement for acoustically transparent materials. In addition, the selective damping of shear modes resulting from CNT additions will enhance the acoustic transparency of monolithic composites at a wide range of incidence angles. Optimized processing methods for CNT dispersion will more fully exploit the reinforcing efficiency and selective damping

potential of CNT composites for underwater sonar structural materials.

Acknowledgements: The authors are grateful for the financial assistance received from the SBIR Navy research funds (Topic No. N06-084) for this project. We thank Hongbin Shen and M.C. Gill Corporation for extending their facilities to fabricate the scale-up sample and their valuable inputs during formulation. We also acknowledge Joel Garrelick, Mathew Sneddon and Hugh Saurenman for their invaluable contribution to this project.

References:

1. Thomson, C.M., "Development of a Structurally Rigid, Acoustically Transparent Plastic", Journal of Acoustic Society of America, 87 (1990): 1138-1143.
2. "Acoustic Window", United States Patent 6,831,876
3. Thomas S. Ramotowski, "Rubber-Toughened Epoxies for Acoustical Applications", Master's Thesis, (2003), University of Rhode Island
4. Robert E. Montgomery, Fred J. Weber, and David F. White, "On the Development of Acoustically Transparent Structural Plastics", Journal of Acoustic Society of America,71(1982): 735-741.
5. (a) Twardowski, T.E., and Geil, P.H., "A Highly Fluorinated Epoxy Resin: Post-Curing and Transition Behavior", Journal of Acoustic Society of America, 41(1990):1047-1054. (b) Twarsowski, T.E., and Geil, P.H., "Highly Fluorinated Epoxy Resins. II. Behavior in Blend Applications", Journal of Acoustic Society of America, 42(1991):69-74. (c) Twardowski, T.E., and Geil, P.H., "A Highly Fluorinated Epoxy Resin. III. Behavior in Composite and Fiber-Coating Applications", Journal of Acoustic Society of America, 42(1991): 1721-1726.
6. Wei Chen, Maria L Auad, William R.J.J., Steven R. Nutt, "Improving the dispersion and flexural strength of multiwalled carbon nanotubes–stiff epoxy composites through β-hydroxyester surface functionalization coupled with the anionic homopolymerization of the epoxy matrix", European Polymer Journal, 42 (2006): 2765-2772.
7. Wei Chen, Hongbin Lu, Steven R. Nutt, "The influence of functionalized MWCNT reinforcement on the thermomechanical properties and morphology of epoxy nanocomposites", Composite Science and Technology, DOI: 10.1016/j.compscitech.2008.05.011, In press, available online 21 May 2008
8. Wei Chen, Hongbin Shen, Maria L. Auad, Steven R. Nutt, "Basalt Fiber – Epoxy Laminates with Functionalized Multi-walled Carbon Nanotubes", submitted to Composites Science and Technology, (2008), under review.
9. Jonghwan Suhr, Nikhil Koratkar, Pawel Keblinski, and Pulickel Ajayan, "Viscoelasticity in Carbon Nanotube Composites", Nature Materials, 4(2005):134-137.
10. Koratkar, N.A. et al, "Carbon Nanotube Films for Damping Applications", Advanced Materials, 14(2002): 997-1000.

11. Salvetat, J. P. et al, "Mechanical Properties of Carbon Nanotubes", Applied Physics A, 68(1999): 287-292.
12. Koratkar, N.A. et al, "Multifunctional Structural Reinforcement Featuring Carbon Nanotube Films", Composite Science and Technology, 63(2003):1525-1531.
13. Liu, L. and Wagner, H. D., "Rubbery and Glassy Epoxy Resins Reinforced with Carbon Nanotubes", Composites Science and Technology, 65(2005):1861-1868.
14. Jihua Gou, Scott O'Braint, Haichang Gu, and Gangbin Song, "Damping Augmentation of Nanocomposites Using Carbon Fiber Paper", Journal of Nanomaterials, 32803(2006):1-7.
15. Loana C. Finegan, Gary G. Gibbetts, and Ronald F. Gibson, "Modeling and characterization of damping in carbon nanofiber/polypropylene composites", Composites Science and Technology, 63(2003):1629-1635.
16. Dasgupta, A. (Dept. of Mech. Eng., Maryland Univ., College Park, MD, USA); Bhandarkar, S.M., "A generalized self-consistent Mori-Tanaka scheme for fiber-composites with multiple interphases", Mechanics of Materials, 14 (Nov. 1992):p 67-82
17. Chatterjee, A.P. "A model for the elastic moduli of three-dimensional fiber networks and nanocomposites", Journal of Applied Physics, 100 (Sept. 2006):54302-1-8
18. D'Almeida, J.R.M., "An Analysis of the Effect of the Diameters of the Glass Microspheres on the Mechanical Behavior of Glass-Microsphere/Epoxy-Matrix Composites", Composite Science and Technology, 59(1999): 2087-2091.